

Harnessing the giant out-of-plane Rashba effect and the nanoscale persistent spin helix via ferroelectricity in SnTe thin films

Hosik Lee,^{1,*} Jino Im,^{2,*} and Hosub Jin^{3,†}

¹*School of Mechanical, Aerospace and Nuclear Engineering,*

Ulsan National Institute of Science and Technology (UNIST), Ulsan 44919, Korea

²*Center for Molecular Modeling and Simulation, Korea Research Institute of Chemical Technology, Daejeon 34114, Korea*

³*Department of Physics, Ulsan National Institute of Science and Technology (UNIST), Ulsan 44919, Korea*

A non-vanishing electric field inside a non-centrosymmetric bulk crystal transforms into a momentum-dependent magnetic field, namely, a spin-orbit field (SOF). SOFs are of great use in spintronics because they enable spin manipulation via the electric field. At the same time, however, spintronic applications are severely limited by the SOF, as electrons traversing the SOF easily lose their spin information. Here, we propose that in-plane ferroelectricity in (001)-oriented SnTe thin films harness the Janus-faced SOF in a reconcilable way to enable electrical spin controllability and suppress spin dephasing. The in-plane ferroelectricity produces a unidirectional *out-of-plane Rashba* SOF that can host a long-lived helical spin mode known as a persistent spin helix (PSH). Through direct coupling between the inversion asymmetry and the SOF, the ferroelectric switching reverses the out-of-plane Rashba SOF, giving rise to a maximally field-tunable PSH. Furthermore, the giant out-of-plane Rashba SOF seen in the SnTe thin films is linked to the nano-sized PSH, potentially reducing spintronic device sizes to the nanoscale. We combine the two ferroelectric-coupled degrees of freedom, longitudinal charge and transverse PSH, to design intersectional electro-spintronic transistors governed by non-volatile ferroelectric switching within nanoscale lateral and atomic-thick vertical dimensions.

The spin-orbit field (SOF) induced by inversion asymmetry has been an important factor in spintronics [1–3] ever since the development of the Datta–Das spin field-effect transistor [4–6], which harnesses the coherent spin precession controlled by the Rashba SOF [7]. Although not unheard of, however, the SOF is rarely compatible with long spin lifetimes because it breaks the spin rotational symmetry and suffers from fast spin decoherence in a diffusive transport regime [8]. Thus, acquiring electrical spin controllability while preserving the long spin coherence has been elusive. As an exceptional example, the unidirectional SOF emerges from the interplay between Rashba and Dresselhaus SOFs in III-V semiconductor quantum wells of general crystal orientation and enables coherent spin manipulation by hosting the persistent spin helix (PSH), with a lifetime of a few nanoseconds [9–14]. However, the small and finely tuned SOF strengths in III-V semiconductor heterostructures have presented a bottleneck in practical applications. Satisfying the stringent conditions for fine-tuning the Rashba and Dresselhaus SOFs can complicate the attainment of the unidirectional SOF and the corresponding PSH. Even after achieving the unidirectional SOF and PSH, efficient spin manipulation via the electric field is limited by the small values and narrow ranges available to the Rashba and Dresselhaus terms. The small SOF then generates a micrometer-long pitch in the PSH, hampering the ability to fabricate small spin transistors for high-density and scalable spintronic devices [15].

In pursuit of a better spin transport device, the present work sought an easily accessible and controllable PSH with rapid precession in space and a slow decay in the time domain. The ideal target system should exhibit a unidirectional, field-tunable, large SOF driven by a single inversion asymmetry. Instead of dealing with the fine-tuned Rashba and Dresselhaus terms, the in-plane electric field in a two-dimensional electron

system can simply produce a unidirectional SOF. Given that the SOF generated by the constant electric field is expressed by

$$\vec{\Omega}_{\text{SOF}}(\vec{k}) = \alpha(\hat{E} \times \vec{k}) \quad (1)$$

up to the leading order in the electron momentum \vec{k} , a variety of SOFs are possible, depending on the field direction. (Here, α is a system-dependent coefficient multiplied by the field strength, and \hat{E} denotes the field direction.) Application of the in-plane electric field, say $\hat{E} \parallel +\hat{x}$, yields an SOF with the following form:

$$\vec{\Omega}_{\text{SOF}}(\vec{k}) = \alpha(\hat{x} \times \vec{k}) = \alpha k_y \hat{z}. \quad (2)$$

The SOF induced by the in-plane electric field shows unidirectional alignment perpendicular to the plane, which has an identical form in the III-V quantum well grown along the [110] direction [13]. This SOF may be referred to as the out-of-plane Rashba effect, in contrast with the conventional Rashba effect that has in-plane SOF components [7] (see Fig. 1(a)). Combining the unidirectional Rashba SOF with the quadratic kinetic energy yields the Hamiltonian $\mathcal{H} = \mathcal{H}_{\text{kin}} + \vec{\Omega}_{\text{SOF}} \cdot \vec{\sigma} = \frac{\hbar^2}{2m}(k_x^2 + k_y^2) + \alpha k_y \sigma_z$, where $\vec{\sigma}$ denotes the Pauli spin matrices. The in-plane electric field induces the two-dimensional parabolic band to undergo an out-of-plane Rashba effect, leading to a spin texture identical to that seen in the equivalent Rashba and Dresselhaus system, except for the spin quantization axis. Spin-up and spin-down parabolic bands are shifted by a constant vector $\vec{Q} = \frac{2m\alpha}{\hbar^2} \hat{y}$, and a spin-degenerate line node appears along the $k_y = 0$ momenta parallel to the field direction.

When incorporated into the ferroelectricity, the in-plane electric field becomes accessible in a fully controllable manner. The in-plane ferroelectricity naturally develops an in-

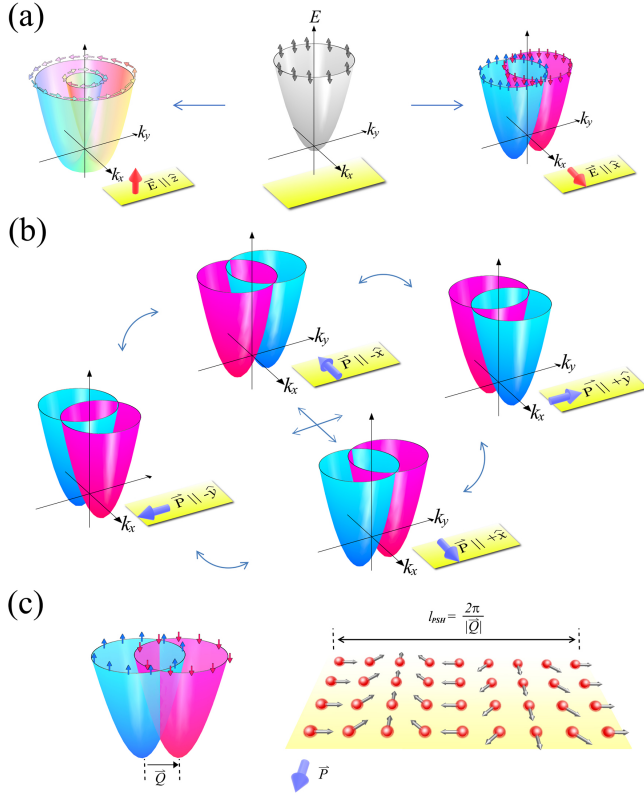


FIG. 1. (a) In a two-dimensional electron system, the conventional and out-of-plane Rashba spin-orbit fields (SOFs) appear under the out-of-plane and in-plane electric fields, respectively. (b) The out-of-plane Rashba band induced by the in-plane ferroelectricity represents the maximally controllable SOF, depending on the ferroelectric configurations. (c) The out-of-plane Rashba SOF shifts the spin-up and spin-down parabolic bands by a constant vector \vec{Q} , which hosts the long-lived PSH with a spatial periodicity $\frac{2\pi}{|\vec{Q}|}$.

plane electric field and produces a unidirectional and maximally field-tunable Rashba SOF from a single inversion asymmetry. In general, the SOF induced by the ferroelectric polarization can be written as [16, 17]

$$\vec{\Omega}_{\text{SOF}}(\vec{k}) = \alpha(\hat{P} \times \vec{k}),$$

where \hat{P} , the polarization direction, replaces \hat{E} in Eq. (1). Here, $\vec{\Omega}_{\text{SOF}}$ is completely locked on the ferroelectric polarization. Once again, if \hat{P} is parallel to the plane, the unidirectional Rashba SOF described in Eq. (2) emerges, but with direct ferroelectric coupling. The ferroelectric-coupled out-of-plane Rashba SOF changes its sign by switching its polarization. Moreover, a rich variety of controlled SOFs is anticipated, depending on the ferroelectric domain structure. For example, in a target system composed of a square-based lattice, four 90° -rotated configurations of the in-plane ferroelectric moment are possible, and the out-of-plane Rashba SOF can vary accordingly (Fig. 1(b)).

As observed in the equivalent Rashba and Dresselhaus system, the out-of-plane Rashba band, in which the spin-up and

spin-down bands are shifted by a constant vector \vec{Q} , is known to host the long-lived PSH by recovering the spin rotational SU(2) symmetry [10]. Injection of electron spin aligned with the plane induces precession of the spin around the z -axis with a spatial periodicity of $l_{\text{PSH}} \equiv \frac{2\pi}{|\vec{Q}|} = \frac{\pi\hbar^2}{m\alpha}$ (Fig. 1(c)). In a practical application of the out-of-plane Rashba effect, the coherent spin precession of the PSH can be exploited to fabricate a spin transistor with a size that is determined by l_{PSH} [9, 18, 19]. Because small spin transistors are required for the development of high-density scalable spintronic devices [15], the short pitch size of a rapidly precessing PSH is highly desirable. A small l_{PSH} requires a large Rashba coefficient α ; therefore, target two-dimensional ferroelectric materials would likely consist of heavy elements that possess large atomic spin-orbit coupling.

A (001)-oriented atomically thin SnTe film, recently synthesized using molecular beam epitaxy [20], is the most promising material potentially capable of satisfying the above criteria to produce a unidirectional, field-tunable, and extremely large SOF driven by a single inversion asymmetry. To verify this idea, we have performed density functional theory calculations, and found that the Heyd-Scuseria-Ernzerhof functional [21] well describes experimental ferroelectric dis-

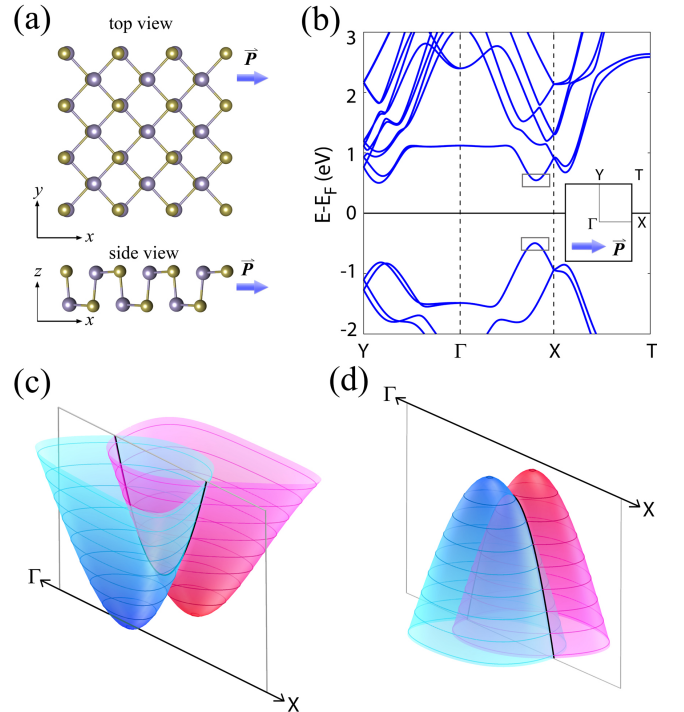


FIG. 2. (a) Crystal and (b) electronic structures of the 1-unit-cell-thick SnTe film. Sn and Te atoms are colored blue and yellow, respectively. Ferroelectric-coupled out-of-plane Rashba bands emerged both at (c) the conduction band minimum (CBM) and (d) the valence band maximum (VBM). Spin-degenerate line nodes indicated by black solid lines in (c) and (d) correspond to the parabolic bands inside the grey box in (b). The interval between each contour line is 15 meV.

placements. For computational details and discussions on the lattice optimization, see the Supplemental Material. As shown in Fig. 2(a), rock-salt based SnTe thin films display opposing displacements of the tin and tellurium atoms within a plane, resulting in ferroelectric distortion parallel to the two-dimensional plane. The overall electronic band structure of a one-unit-cell-thick SnTe film is shown in Fig. 2(b). The conduction and valence band edges appear on the line Γ -X in the Brillouin zone, along which the ferroelectric polarization is aligned. No spin splitting occurs near the band edges on the line Γ -X because this line corresponds to the spin-degenerate line node seen in the out-of-plane Rashba SOF. By observing the low-energy electronic spectrum, the out-of-plane Rashba band structures emerge, as shown in Figs. 2(c) and 2(d). Away from the spin-degenerate line Γ -X, spin splitting appears such that the spin direction at each spin split-off band is normal to the SnTe film. In other words, the unidirectional SOF enforces the out-of-plane spin texture. The contour plot of the spin split-off bands reveals that the spin-up and spin-down bands close to each band edge overlap with a constant shift, confirming the existence of a ferroelectric-coupled out-of-plane Rashba SOF in the SnTe thin films. (For electronic structures of SnTe thin films with different thicknesses, see the Supplemental Material.)

In contrast to the conventional Rashba SOF, in which the time-reversal symmetry protects the spin degeneracy at $\vec{k} = 0$, extra symmetries are needed to realize an out-of-plane Rashba SOF in a crystalline solid. The lattice symmetry should be compatible with the unidirectional spin texture and the spin-degenerate line node seen in the out-of-plane Rashba band. Two mirror symmetries in a two-dimensional bulk crystal lacking inversion symmetry may be a simple recipe for achieving an out-of-plane Rashba SOF. The system should be invariant under both in-plane mirror and vertical mirror reflections (say \mathcal{M}_{xy} and \mathcal{M}_{zx} , respectively). The unidirectional SOF is protected by \mathcal{M}_{xy} because only the out-of-plane SOF component, Ω_{SOF}^z , survives under the in-plane mirror reflection. In addition, \mathcal{M}_{zx} regulates Ω_{SOF}^z as an odd function under the vertical mirror reflection; i.e., $\Omega_{\text{SOF}}^z(-k_y) = -\Omega_{\text{SOF}}^z(k_y)$. (For more details, see the Supplemental Material.) Therefore, Ω_{SOF}^z is zero along the line $k_y = 0$, and the spin-degenerate line node emerges along the intersection between the two mirror planes. The in-plane ferroelectricity that coexists with two perpendicular mirror planes could potentially provide a design principle guiding the implementation of a ferroelectric-coupled out-of-plane Rashba SOF. In SnTe thin films, vertical mirror symmetry and an in-plane mirror reflection exist in combination with the half-unit-cell translation to constitute a unidirectional SOF and a spin-degenerate line node [22]. Symmetry protection renders the SnTe thin films robust in their access to the out-of-plane Rashba SOF.

The salient features of SnTe thin films for applications are illustrated in Fig. 3. Importantly, the giant Rashba coefficients α of 1.28 – 2.85 eVÅ are present in both the conduction and valence band edges (Fig. 3(a)). These coefficients are two to three orders of magnitude larger than those in the III-V semi-

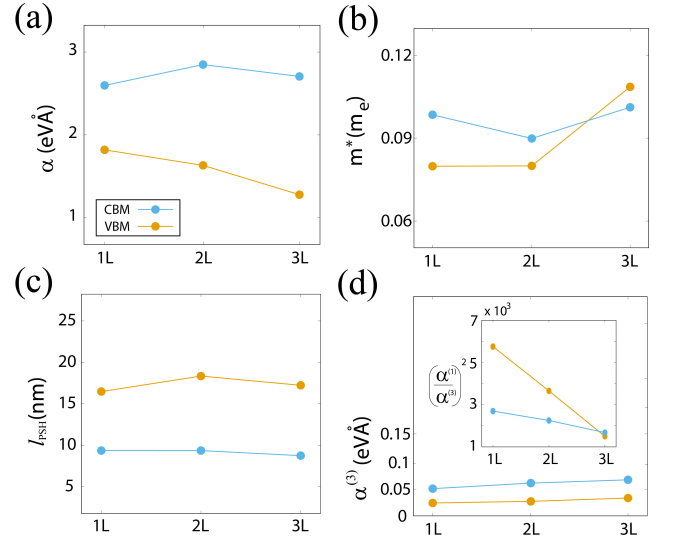


FIG. 3. (a) The out-of-plane Rashba coefficient, (b) effective mass, (c) pitch size of PSH, and (d) k -cube Rashba coefficient at the CBM and VBM. 1L, 2L, and 3L denote one-, two-, and three-unit-cell-thick SnTe films, respectively.

conductor quantum well structures [3, 11]. The giant value of α is attributed to large atomic spin-orbit coupling and ferroelectric distortion in the SnTe thin films. Considering the effective mass shown in Fig. 3(b), the pitch size of the PSH falls within the range 8.8 – 18.3 nm (Fig. 3(c)). A huge reduction in l_{PSH} occurs compared to the III-V semiconductor quantum wells that provided a PSH of a few micrometers in length [11, 12]. Hence, the giant out-of-plane Rashba SOF improves the suitability of this material for use in nano-sized spin transistors by handling the rapid but coherent spin precession of the PSH [15].

The cubic out-of-plane Rashba term, $\alpha^{(3)}$, was estimated to investigate the long lifetime of the PSH in the SnTe thin films (Fig. 3(d)). The higher-order momentum dependence of the SOF could be expressed as

$$\begin{aligned}\Omega_{\text{SOF}}^z(\vec{k}) &= \alpha k_y + \alpha' k_x^2 k_y + \alpha'' k_y^3 \\ &\simeq \alpha^{(1)} k \sin \theta + \alpha^{(3)} k \sin 3\theta,\end{aligned}$$

, where $\alpha^{(1)} = \alpha + \frac{1}{4}(\alpha' + 3\alpha'')\langle k^2 \rangle$, $\alpha^{(3)} = \frac{1}{4}(\alpha' - \alpha'')\langle k^2 \rangle$, and θ indicates the angle of momentum \vec{k} with respect to the x -axis. By analogy to the equivalent Rashba and Dresselhauss system, the main source of spin dephasing in the unidirectional SOF is the k -cube term, which breaks the spin rotational SU(2) symmetry [10, 23]: $D_s \tau_{\text{PSH}} \sim \left(\frac{\hbar^2}{m \alpha^{(3)}} \right)^2$, where D_s is the spin-diffusion constant, and τ_{PSH} is the spin lifetime of the PSH mode [12]. Assuming a carrier concentration $n = k_f^2 / 2\pi = 5 \times 10^{11} \text{ cm}^{-2}$, we estimated $\alpha^{(3)} \simeq \frac{1}{4}(\alpha' - \alpha'') k_f^2$, as plotted in Fig. 3(d). The inset of Fig. 3(d) shows $(\alpha^{(1)} / \alpha^{(3)})^2$, which is linked to the dimensionless quantity $\eta \equiv D_s \tau_{\text{PSH}} |\vec{Q}|^2 \sim (\alpha^{(1)} / \alpha^{(3)})^2$, which

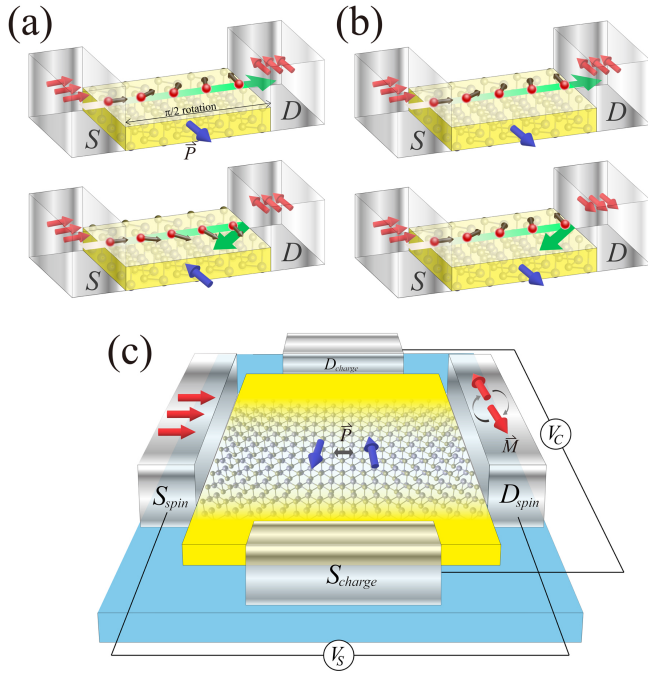


FIG. 4. Two non-volatile on-off switching mechanisms are shown in the spin-valve-like structure, in which a SnTe thin film provides the spin transport channel: (a) electric and (b) magnetic on-off switching. (c) A multi-functional cross-shaped charge-spin transistor.

describes the ratio of the spin relaxation times of the PSH and the ordinary spin diffusion [11]. The known η values in the III-V semiconductors are of the order of 10^2 , and the overall values in the SnTe thin films are $\sim 10^3$, indicating a slowly decaying PSH. By hosting a nanometer-sized and long-lived PSH, the SnTe thin films may serve as an ideal platform for high-density spintronic devices that are immune to spin dephasing.

Considering the availability of non-volatile control over the ferroelectricity, SnTe thin films could enable novel multi-functional spin transistors. As a simple sketch for a device application, a spin-valve-like experimental set-up composed of ferromagnetic electrodes and a SnTe thin film as a transport channel could facilitate two switching modes by employing a ferroelectric-coupled PSH. Ferromagnetic metal leads at both ends would have in-plane and orthogonal spin orientations, and the ferroelectric polarization in the SnTe channel would align perpendicular to the transport direction. The channel length would be set to $l_{\text{PSH}}/4$ (modulo $l_{\text{PSH}}/2$), corresponding to $\pi/2$ (modulo π) spin precession of the PSH. Injection of the spin-polarized electron from the source electrode into the SnTe channel would rotate the traversing spin around the z -axis by $\pi/2$ (modulo π) at the end of the channel [24]. Because the spin configurations of the ferromagnetic source and drain electrodes would be orthogonal, the electron spin at the end of the SnTe channel would be either parallel or antiparallel to the spin orientation of the drain, leading to an on- or off-state, respectively. The on-off switching could be controlled

by flipping either the electric polarization of the SnTe channel (Fig. 4(a)) or the magnetic polarization of the ferromagnetic electrodes (Fig. 4(b)). Combined with the charge switching mechanism along the polarization direction [20], we designed the multi-functional cross-shaped charge-spin transistor sketched in Fig. 4(c). The intersectional charge and spin channels may be simultaneously switched by controlling the electric polarization of the SnTe thin film, or the spin transport may be separately tuned by adjusting the magnetic polarization of the ferromagnetic electrodes.

The unidirectional, ferroelectric-coupled, giant out-of-plane Rashba effect shown in SnTe thin films can provide a new scheme for carrying and manipulating spin information, thereby broadening the scope of current spintronic technologies. The nanometer lateral and atomically thin vertical scale over which the coherent spin is manipulated could enable SnTe thin films to form heterostructures with other two-dimensional materials, such as van der Waals layered compounds [20, 25, 26], rendering them suitable for use in highly integrated multi-functional devices. Additionally, given the superb thermoelectric response of bulk SnTe [27, 28], SnTe thin films could be a fascinating new option for thermo-spintronic applications [29], possibly associating a drift in the PSH to an entropy-carrying degree of freedom under a temperature gradient.

Financial support from the Basic Science Research Program of the National Research Foundation of Korea (NRF) under Grant No. 2016R1D1A1B03933255 (H.J.) and 2017R1D1A1B03028004 (H.L.) is gratefully acknowledged.

* These authors contributed equally to this work.

† Correspondence should be addressed to hsjin@unist.ac.kr

- [1] I. Žutić, J. Fabian, and S. Das Sarma, *Rev. Mod. Phys.* **76**, 323 (2004).
- [2] Y. Kato, R. C. Myers, A. C. Gossard, and D. D. Awschalom, *Nature* **427**, 50 (2004).
- [3] J. Nitta, T. Akazaki, H. Takayanagi, and T. Enoki, *Phys. Rev. Lett.* **78**, 1335 (1997).
- [4] S. Datta and B. Das, *Appl. Phys. Lett.* **56**, 665 (1990).
- [5] H. C. Koo *et al.*, *Science* **325**, 1515 (2009).
- [6] P. Chuang *et al.*, *Nat. Nanotech.* **10**, 35 (2015).
- [7] Y. A. Bychokov and E. I. Rashba, *JETP Lett.* **39**, 78 (1984).
- [8] M. I. Dyakonov and V. I. Perel, *Sov. Phys. Solid State* **13**, 3023 (1972).
- [9] J. Schliemann, J. C. Egues, and D. Loss, *Phys. Rev. Lett.* **90**, 146801 (2003).
- [10] B. A. Bernevig, J. Orenstein, and S.-C. Zhang, *Phys. Rev. Lett.* **97**, 236601 (2006).
- [11] J. D. Koralek *et al.*, *Nature* **458**, 610 (2009).
- [12] M. P. Walser, C. Reichl, W. Wegscheider, and G. Salis, *Nat. Phys.* **8**, 757 (2009).
- [13] J. Schliemann, *Rev. Mod. Phys.* **89**, 011001 (2017).
- [14] M. Kammermeier, P. Wenk, and J. Schliemann *Phys. Rev. Lett.* **117**, 236801 (2016).

- [15] S. Sugahara and J. Nitta, Proc. IEEE **98**, 2124 (2010).
- [16] D. Di Sante, P. Barone, R. Bertacco, and S. Picozzi, Adv. Mater. **25**, 509 (2013).
- [17] M. Kim, J. Im, A. J. Freeman, J. Ihm, and H. Jin, Proc. Natl. Acad. Sci. U.S.A. **111**, 6900 (2014).
- [18] X. Cartoixá, D. Z.-Y. Ting, and Y.-C. Chang, Appl. Phys. Lett. **83**, 1462 (2003).
- [19] Y. Kunihashi *et al.*, Appl. Phys. Lett. **100**, 113502 (2012).
- [20] K. Chang *et al.*, Science **353**, 274 (2016).
- [21] J. Heyd, G. E. Scuseria, and M. Ernzerhof, J. Chem. Phys. **118**, 8207 (2003).
- [22] I. Appelbaum and P. Li, Phys. Rev. B **94**, 155124 (2016).
- [23] T. D. Stanescu and V. Galitski, Phys. Rev. B **75**, 125307 (2007).
- [24] Y. Kunihashi *et al.*, Nat. Commun. **7**, 10722 (2016).
- [25] A. K. Geim and I. V. Grigorieva, Nature **499**, 419 (2013).
- [26] K. S. Novoselov, A. Mishchenko, A. Carvalho, and A. H. Castro Neto, Science **353**, aac9439 (2016).
- [27] L.-D. Zhao *et al.*, Nature **508**, 373 (2014).
- [28] L.-D. Zhao *et al.*, J. Am. Chem. Soc. **138**, 2366 (2016).
- [29] G. E. W. Bauer, E. Saitoh, and B. J. van Wees, Nat. Mater. **11**, 391 (2012).